Phosphorescence and Optically Detected Magnetic Resonance of Polynucleotide Complexes of Tryptophan- and 5-Methyltryptophan-Containing Peptide Stereoisomers

Ajay Misra,[†] Michael Blair,[†,‡] Christina Stuart,[†,‡] Andrzej Ozarowski,[†] Jose R. Casas-Finet,[§] and August H. Maki[†,*]

Department of Chemistry, University of California, Davis, California 95616, and AIDS Vaccine Program, SAIC Frederick, National Cancer Institute-Frederick Cancer Research and Development Center, Frederick, Maryland 21702-1201

Received: October 18, 2001; In Final Form: January 17, 2002

Phosphorescence and optically detected magnetic resonance (ODMR) measurements of tryptophan (W) and 5-methyltryptophan (MeW) triplet states are reported in stereoisomeric peptide complexes with polynucleotides. The peptide diastereomers KWK, K(MeW)K, KGWK, and KGWGK in which the W or MeW are either D or L and the lysine (K) is L have been prepared and their complexes with poly(deoxythymidylic) acid (poly dT), poly(inosinic) acid (poly I), and poly(uridylic) acid (poly U) have been studied. Complex formation with polynucleotide results in a phosphorescence redshift and reduction of the zero field splitting *D* value of W or MeW that varies with polynucleotide, the length and sequence of the peptide, and with the diastereomer. In addition, the kinetic parameters of the triplet state show considerable variation between complexes. These results are discussed in terms of the stereochemistry of peptide bonding to the single stranded polynucleotide and differing types of aromatic amino acid−base interaction: intercalation, aromatic stacking, and edge-to-face contact. Our results are consistent with binding of the peptide to helical regions of the polynucleotide in a single-stranded helical β-sheet structure in which alternating side chains of an all L oliogopeptide face inward toward the bases and outward from the helix. The orientation is determined by the N-terminal lysine that binds in a stereospecific manner to DNA phosphates through its α- and ϵ-amino groups. This model resembles one originally proposed by Gabbay et al. [Gabbay, E. J.; Adawadkar, P. D.; Wilson, W. D. *Biochemistry* **1976**, *15*, 146; Gabbay, E. J.; Adawadkar, P. D.; Kapicak, L.; Pearce, S.; Wilson, W. D. *Biochemistry* **1976**, *15*, 152] for peptide binding to duplex DNA.

Introduction

The functionality of many biological molecules depends on chirality. Although L-amino acids are by far the most predominant enantiomer found, nature provides a number of examples of D-amino acids, as well. Some bacterial peptides, and the amphibian skin peptides, dermorphin and deltorphin, that are related to mammalian hormones and neurotransmitters contain D-amino acids.[1] Also, free D-amino acids are present in mammalian tissues and body fluids.[2,3]

The evolutionary sequence that has led to the contemporary highly specific translation of genetic material to protein has remained elusive.[4] A model of chemically selective amino acid−nucleic acid association has been formulated,[5,6] and model studies[7] have suggested that even small preferences in the interaction of nucleic acid with different amino acids could lead eventually to an accurate translation system. Stereoselectivity in amino acid−nucleic acid interactions has received much attention. Wickramasinghe et al.[8] studied the relative rates of esterification of 5′-AMP, a D-ribose nucleotide, by enantiomeric amino acids, and found a preference for the D-amino acid that increases with hydrophobicity, suggesting that hydrophobic interaction between adenine and the amino acid side chain is stereoselective. This selectivity is reversed in esterification of dipeptides, however, where the L,L enantiomer is preferred over D,D.[9] L-Amino acid derivatives have been found[10] to raise the melting temperature of duplex RNA more than the corresponding D enantiomers, suggesting stereospecific peptide−nucleic interactions.

Interactions between mononucleotides and aromatic amino acid esters are very weak,[11,12] with $K_a \sim 10\ M^{-1}$ or less. L-Tryptophan (W) binds to mononucleotides with the following order of affinities: UMP ∼ CMP < GMP < AMP.[12] W binds to AMP with slightly greater affinity than does D-tryptophan (W*).[12] (A D-amino acid will be designated by adding * to its symbol.) The extent of association between W and nucleic acids is enhanced in aggregates formed in frozen aqueous solution, where quenching of W fluorescence is attributed to aromatic stacking between the indole chromophore and nucleobase.[13,14] The introduction of basic amino acids such as lysine (K) to form W-containing peptides increases the binding affinity of nucleic acids and enables the study of DNA and RNA complexes of peptides such as lysyltryptophanyllysine (KWK) in dilute aqueous solution using fluorescence quenching of W.[15−18] Fluorescence quenching measurements can be interpreted in terms of two limiting types of complex, an "externally bound" complex that exhibits normal fluorescence quantum yields and lifetimes, and a second complex in which W is stacked or intercalated with bases and whose fluorescence is

* Telephone: (530) 752-6471. Fax: (530) 752-8995. E-mail: maki@indigo.ucdavis.edu.

[†] University of California, Davis.

[‡] Partially supported by the Camille and Henry Dreyfus Foundation through a Senior Scientist Mentor Initiative Award to A.H.M.

[§] AIDS Vaccine Program, SAIC Frederick. Present address: Medimmune, Inc., 35 West Watkins Road, Gaithersburg, MD 20878.

10.1021/jp013879t CCC: $22.00
Published on Web 03/07/2002

completely quenched.[19] The sequential formation of externally bound and stacked complexes has been confirmed by electric field jump kinetics measurements of KWK binding to calf thymus DNA.[20] Specific effects of base stacking of aromatic amino acid-containing peptides on the circular dichroism of poly(riboadenylic) acid (poly A) and other helical polyribonucleotides have been reported,[21] as well as proton NMR shifts caused by stacking-induced ring currents.[22,23] The binding of KWK to poly A also has been studied using optically detected magnetic resonance (ODMR).[24] Shifts in the zero field splitting (zfs) parameters of W in its excited triplet state are attributed to stacking interactions with bases. Zfs shifts, phosphorescence shifts, and phosphorescence lifetime reduction of specific W residues of *E. coli* single-stranded DNA binding protein (Eco SSB) are induced by base stacking in poly(deoxythymidylic) acid (poly dT) complexes.[25,26] Mascotti and Lohman[27,28] carried out studies of the binding thermodynamics of a series of oligolysines containing one, two, or three W residues with several single-stranded polynucleotides. The binding affinity increases with W content, demonstrating the stabilization conferred by aromatic stacking interactions. Binding of the tetrapeptides KWGK and KGWK to a series of polynucleotides has been investigated.[29,30] Stacking interactions are greater with single-stranded than duplex substrates. In addition, complex formation of KWK, KGWK(*O-tert*-butyl ester), and KGWGK, with DNA hairpins and duplexes reveal various degrees of aromatic stacking.[31,32]

The peptide−nucleic acid binding studies outlined above have been carried out using the naturally occurring L-amino acids. Peptides such as KWK and KW*K are diastereomers that would be expected to bind in a different manner to polynucleotides. The binding of KF (F is phenylalanine) and KF* to salmon sperm DNA has been compared[33] with the result that aromatic stacking of KF exceeds that of KF*. Similar studies of the binding of K(5FW)K and K(5FW*)K (5FW is 5-fluorotryptophan) to duplex DNA[34] and DNA containing apurinic lesions[35] shows that fluorine is partially inserted into the base stack in the K(5FW)K complex, while there is no interaction of fluorine with bases in the K(5FW*)K complex. In this communication, we will use phosphorescence and ODMR spectroscopy to compare complexes formed between three polynucleotides [poly dT, poly(uridylic) acid (poly U), and poly(inosinic) acid (poly I)] and resolved peptide diastereomers that contain a single aromatic amino acid, W or 5-methyltryptophan (MeW). The four peptide diastereomer pairs investigated are the following: KWK, KW*K; K(MeW)K, K(MeW*)K; KGWK, KGW*K; and KGWGK, KGW*GK. This study focuses on the effects of nucleic acid binding on the triplet state properties of the aromatic amino acid as determined by ODMR and phosphorescence measurements. Of particular interest is the effect of stereoisomerism of the aromatic amino acid, the length and sequence of the peptide, the specific polynucleotide, and 5-methylation of W on triplet state properties as determined from phosphorescence and ODMR spectra. In previous work,[36−38] we have shown that the triplet state energy, the zfs parameters, the populating rates, and decay kinetics of W are sensitive to local interactions, including aromatic stacking with bases.

Experimental Section

Poly dT, poly U, and poly I were purchased as lyophilized samples from Pharmacia. All W-containing peptides were synthesized by Macromolecular Resources (Fort Collins, CO) as separate stereoisomers, purified to better than 90% by reverse-phase HPLC, and assessed by MALDI mass spectroscopy. The K(MeW)K and K(MeW)*K peptides were synthesized by Peptide Technologies (Gaithersburg, MD) as the racemic mixture, separated and purified by reverse phase HPLC, and assessed by MALDI MS. The stereoisomers were identified by comparison of their CD spectra with those of KWK and KW*K. Peptides and polynucleotides were dissolved in deionized, doubly distilled water. Complexes were formed by adding an aliquot of peptide solution and mixing for 1 h. Ethylene glycol (EG) was added as cryosolvent to 40% v/v. The final peptide concentration was 0.4 mM, and the polynucleotide was in 10-fold excess (monomer basis). Samples, ca. 40 μL, were introduced into 2 mm inner diameter Spectrasil quartz tubes for phosphorescence and ODMR measurements.

The phosphorescence/ODMR spectrometer that employs photon counting has been described previously.[39,40] Phosphorescence measurements were made at 77 and 4.2 K with excitation by a 100 W high-pressure Hg arc lamp whose output was filtered through a 0.1 m monochromator using 16 nm band-pass. Glass filters were used to limit further the excitation band. Phosphorescence was viewed through a rotating sector with a delay period of 1 ms and dispersed by a 1 m monochromator. ODMR measurements were carried out in zero applied magnetic field at 1.2 K in order to minimize spin−lattice relaxation (SLR). The 0,0-band of the W or MeW phosphorescence was monitored using a 3 nm band-pass. Delayed slow-passage ODMR measurements were made during the decay of phosphorescence and analyzed as described earlier[41] to obtain the band center frequency, ν_0, and bandwidth, $\nu_{1/2}$ (half width at half-maximum intensity, hwhm), of the ODMR signal that is assumed to have a Gaussian shape. Signal accumulation was begun after a delay, t_0, following the closing of the excitation shutter; the microwave frequency sweep was begun after a 2−3 s additional delay to accumulate baseline. For W, the zfs parameters, D and E, were obtained from the two lowest frequency transitions, $D-E$ and $2E$, that are well resolved. For MeW, on the other hand, these transitions overlap, and cannot be spectrally resolved. In this case, we use delayed slow-passage ODMR to observe the highest frequency $D+E$ transition, while the $D-E$ transition is observed with delay sufficiently long that the $2E$ transition no longer contributes to the response. With sufficient delay, only the longest-lived T_z (z is out-of-plane) sublevel is populated, and only the $D+E$ ($T_z \leftrightarrow T_y$) or $D-E$ ($T_z \leftrightarrow T_x$) transition is observed. In tryptophan, the principal x-axis is approximately normal to that of the $C_{2-}C_3$ double bond.[42]

Kinetic and radiative parameters of the triplet state were obtained from microwave-induced delayed phosphorescence (MIDP)[43] data sets, using a global analysis procedure described previously.[40] If MIDP data from at least two of the ODMR transitions (ca. 15 000 data points) are analyzed globally, reliable values for the individual sublevel decay constants, k_i, relative radiative rate constants, $R_{ix} = k_i^r/k_x^r$, SLR rate constants, W_{ij}, and relative sublevel populating rates, P_i (i,j = x, y, z), are obtained.[40] The analysis program has been modified for MeW in which the $D-E$ and $2E$ transitions overlap and cannot be accessed individually. The two MIDP data sets analyzed globally are the $D+E$ set, and a set consisting of simultaneous saturation of the $D-E$ and $2E$ transitions.

Results

Phosphorescence Spectra. The phosphorescence spectra of KWK and its complexes with poly dT, poly I, and poly U are shown in Figure 1. The 0,0-band of tryptophan is shifted to the red in each of the complexes, and their spectra are somewhat broadened. Similar spectra are exhibited by KW*K and its

TABLE 1: Triplet State Spectroscopic Properties of Tryptophan Peptides and Their Polynucleotide Complexes[a]

		D−E		2*E*				
sample	$\lambda_{0,0}$ (nm)	ν_0 (GHz)	$\nu_{1/2}$ (M Hz)	ν_0 (GHz)	$\nu_{1/2}$ (MH z)	*D* (GHz)	*E* (GHz)	$10^6\ \Delta D/\ \Delta E_{0,0}$
KWK	406.8	1.765(1)	61.8(3)	2.493(1)	127(2)	3.011	1.246	
KWK + poly dT	411.1	1.678(1)	65(2)	2.558(6)	140(3)	2.957	1.28	7
KWK + poly I	413.1	1.642(7)	74(1)	2.559(9)	197(14)	2.922	1.28	8
KWK + poly U	412.9	1.688(5)	86(1)	2.49(1)	171(2)	2.93	1.24	7
KW*K	407.7	1.738(1)	62.1(5)	2.56(1)	133(2)	3.02	1.28	
KW*K + poly dT	410	1.706(1)	63.1(6)	2.495(7)	122(1)	2.954	1.25	16
KW*K + poly I	410.5	1.695(3)	78(8)	2.53(2)	149(7)	2.96	1.26	12
KW*K + poly U	408.9	1.717(1)	68(1)	2.524(4)	130(4)	2.979	1.26	19
KGWK	408.8	1.735(1)	66(1)	2.523(3)	131(9)	2.997	1.261	
KGWK + poly dT	410.2	1.6705(5)	57(1)	2.612(2)	130.5(6)	2.976	1.306	8
KGWK + poly I	411.8	1.679(2)	73(2)	2.538(7)	150(10)	2.95	1.269	9
KGWK + poly U	413.1	1.658(3)	84(4)	2.520(5)	172(10)	2.92	1.26	10
KGW*K	408.9	1.712(1)	53.3(8)	2.575(5)	120(2)	3.00	1.287	
KGW*K + poly dT	411.6	1.691(1)	62.8(8)	2.457(9)	98(9)	2.92	1.228	16
KGW*K + poly I	412.4	1.659(1)	68.2(4)	2.55(1)	162(14)	2.93	1.27	11
KGW*K + poly U	415.2	1.611(4)	69(4)	2.57(1)	128(17)	2.89	1.28	9
KGWGK	409	1.718(1)	58.7(4)	2.57(1)	136(2)	3.00	1.28	
KGWGK + poly dT	410.8	1.685(1)	63(1)	2.60(3)	165(7)	2.98	1.30	6
KGWGK + poly I	412.4	1.659(1)	73(1)	2.53(1)	169(8)	2.92	1.26	13
KGWGK + poly U	412.6	1.662(2)	66(3)	2.56(4)	128(10)	2.94	1.28	9
KGW*GK	408.5	1.753(2)	61(2)	2.518(7)	132(6)	3.01	1.26	
KGW*GK + poly dT	411.6	1.691(2)	74(1)	2.52(1)	164(9)	2.95	1.26	11
KGW*GK + poly I	412.6	1.659(1)	74(2)	2.492(6)	190(7)	2.90	1.24	15
KGW*GK + poly U	414.9	1.591(1)	73(1)	2.52(2)	159(10)	2.85	1.26	14

[a] Standard deviations in the last digit are given in parentheses.

TABLE 2: Triplet State Spectroscopic Properties of 5-Methyltryptophan Peptides and Their Polynucleotide Complexes[a]

		|D|-|E|		D+E				
sample	$\lambda_{0,0}$ (nm)	ν_0 (GHz)	$\nu_{1/2}$ (M Hz)	ν_0 (GHz)	$\nu_{1/2}$ (MH z)	|*D*| (GHz)	|*E*| (GHz)	$10^6\ \Delta D/\Delta E_{0,0}$
K(MeW)K	414.2	1.979(6)	127(5)	3.909(7)	78(2)	2.944	0.965	
K(MeW)K + poly dT	417.3	1.899(8)	138(7)	3.854(7)	111(4)	2.876	0.978	12
K(MeW)K + poly I	419.7	1.871(3)	134(2)	3.857(7)	144(4)	2.864	0.993	8
K(MeW)K + poly U	421.8	1.79(1)	181(4)	3.88(2)	124(7)	2.84	1.04	8
K(MeW*)K	414.8	1.957(2)	102(2)	3.901(2)	73(1)	2.929	0.971	
K(MeW*)K + poly dT	416.6	1.902(2)	127(2)	3.873(3)	93(1)	2.887	0.985	13
K(MeW*)K + poly I	416.7	1.915(4)	125(6)	3.882(4)	136(15)	2.899	0.984	9
K(MeW*)K + poly U	421.3	1.759(3)	92(7)	3.96(1)	133(3)	2.86	1.10	6

[a] Standard deviation in the last digit is given in parentheses.

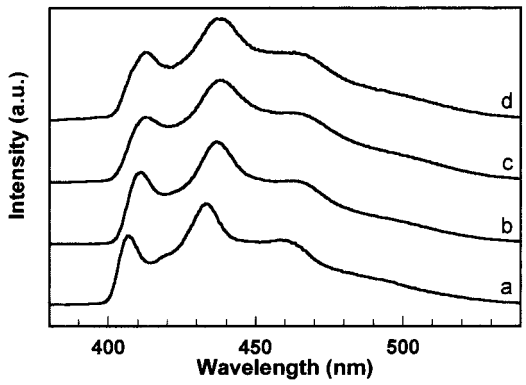

Figure 1. Phosphorescence spectra of (a) KWK, (b) KWK + poly dT, (c) KWK + poly I, and (d) KWK + poly U in 40% v/v EG−water glass at 4.2 K. Samples are excited at 297 nm with 16 nm bandwidth and observed with 3.2 nm resolution.

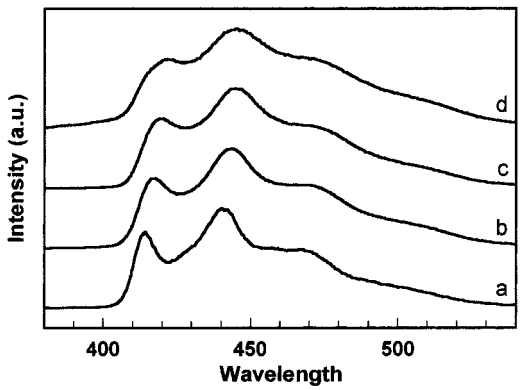

Figure 2. Phosphorescence spectra of (a) K(MeW)K, (b) K(MeW)K + poly dT, (c) K(MeW)K + poly I, and (d) K(MeW)K + poly U in 40% v/v EG−water glass at 4.2 K. Samples are excited at 297 nm with 16 nm bandwidth and observed with 3.2 nm resolution.

polynucleotide complexes, but the spectral redshifts of these complexes are significantly smaller than those found with KWK. All spectra display the characteristic well-resolved vibronic structure of tryptophan. The phosphorescence of each tryptophan-containing peptide is shifted to the red in the presence of polynucleotide, confirming that a complex is formed. The 0,0-band positions of the tryptophan-containing peptides and their polynucleotide complexes are given in Table 1. The phosphorescence spectra of K(MeW)K and its polynucleotide complexes are shown in Figure 2. The spectra show well-resolved vibronic structure similar to tryptophan, and the complexes are redshifted relative to the free peptide. The 0,0-band positions of K(MeW)K, K(MeW*)K, and their polynucleotide complexes are given in Table 2. Methylation at position 5 of tryptophan leads to a ca. 7 nm phosphorescence redshift that is clearly visible in the spectra of the free peptides.

Delayed Slow-Passage ODMR. A typical delayed slow-passage ODMR spectrum of the *D*−*E* transition of the KWK complex with poly U is shown in Figure 3. The superimposed

TABLE 3: Kinetic and Radiative Parameters of Tryptophan Peptides and Their Polynucleotide Complexes[a]

sample	k_x (s^{-1})	k_y (s^{-1})	k_z (s^{-1})	R_{zx}	R_{yx}	W_{xy} (s^{-1})	W_{xz} (s^{-1})	W_{yz} (s^{-1})	P_x[b]	P_y[b]
KWK	0.343(7)	0.113(4)	0.000(2)	0.000(8)	0.094 (7)	0.007(2)	0.027(4)	0.0469(4)	0.43	0.48
KWK + poly dT	0.420(6)	0.119(3)	0.000(2)	0.000(6)	0.064 (5)	0.018(2)	0.029(3)	0.0472(4)	0.55	0.38
KWK + poly I	0.51(2)	0.102(9)	0.000(7)	0.00(1)	0.07(1)	0.029(8)	0.03(1)	0.037(1)	0.65	0.28
KWK + poly U	0.456(9)	0.132(5)	0.000(4)	0.000(9)	0.116 (8)	0.000(3)	0.029(5)	0.0354(6)	0.61	0.32
KW*K	0.325(6)	0.106(3)	0.000(2)	0.000(7)	0.074 (6)	0.013(2)	0.027(3)	0.0465(3)	0.42	0.48
KW*K + poly dT	0.371(6)	0.113(3)	0.000(2)	0.000(7)	0.096 (6)	0.016(2)	0.024(3)	0.0482(4)	0.59	0.33
KW*K + poly I	0.44(1)	0.100(6)	0.000(4)	0.00(1)	0.05(1)	0.040(5)	0.032(7)	0.0518(9)	0.62	0.30
KW*K + poly U	0.38(1)	0.113(6)	0.000(4)	0.00(1)	0.07(1)	0.017(4)	0.030(6)	0.0456(6)	0.56	0.36
KGWK	0.351(9)	0.106(4)	0.004(2)	0.000(9)	0.098 (8)	0.011(3)	0.034(4)	0.0372(4)	0.43	0.48
KGWK + poly dT	0.383(4)	0.107(2)	0.000(1)	0.004(4)	0.022 (4)	0.339(2)	0.025(2)	0.0417(3)	0.64	0.39
KGWK + poly I	0.38(1)	0.105(4)	0.000(2)	0.000(8)	0.058 (7)	0.041(4)	0.036(5)	0.0491(6)	0.45	0.48
KGWK + poly U	0.39(1)	0.112(7)	0.000(5)	0.00(1)	0.04(1)	0.040(5)	0.028(7)	0.0402(9)	0.53	0.39
KGW*K	0.340(5)	0.108(2)	0.004(1)	0.016(4)	0.080 (4)	0.013(1)	0.019(2)	0.0438(2)	0.42	0.49
KGW*K + poly dT	0.380(5)	0.123(3)	0.000(2)	0.004(5)	0.084 (5)	0.029(2)	0.027(3)	0.0474(4)	0.49	0.44
KGW*K + poly I	0.420(7)	0.119(4)	0.000(3)	0.005(8)	0.089 (7)	0.014(3)	0.022(4)	0.0460(4)	0.54	0.39
KGW*K + poly U	0.480(8)	0.127(5)	0.010(4)	0.021(8)	0.127 (7)	0.001(3)	0.019(4)	0.0301(6)	0.66	0.27
KGWGK	0.342(5)	0.115(3)	0.000(2)	0.000(6)	0.109 (5)	0.003(2)	0.027(3)	0.0457(3)	0.40	0.50
KGWGK+ poly dT	0.384(8)	0.113(4)	0.000(3)	0.000(8)	0.091 (7)	0.027(3)	0.032(4)	0.0449(5)	0.56	0.37
KGWGK + Poly I	0.40(2)	0.101(7)	0.000(4)	0.00(2)	0.07(1)	0.051(7)	0.044(9)	0.056(1)	0.55	0.37
KGWGK + Poly U	0.432(8)	0.118(5)	0.000(3)	0.000(8)	0.079 (7)	0.023(3)	0.035(4)	0.0302(5)	0.64	0.28
KGW*GK	0.33(1)	0.108(6)	0.000(3)	0.00(1)	0.09(1)	0.014(4)	0.030(6)	0.0495(6)	0.39	0.51
KGW*GK + poly dT	0.39(1)	0.108(6)	0.002(4)	0.00(1)	0.11(1)	0.016(5)	0.034(7)	0.0456(7)	0.57	0.36
KGW*GK + poly I	0.42(1)	0.111(3)	0.001(2)	0.000(8)	0.043 (7)	0.032(3)	0.029(4)	0.0477(5)	0.64	0.29
KGW*GK + poly U	0.47(1)	0.112(9)	0.005(7)	0.00(1)	0.12(1)	0.002(7)	0.029(9)	0.0296(8)	0.66	0.26

[a] Standard deviation in the last digit is given in parentheses. [b] Estimated error in P_x and P_y is ± 0.03. See text.

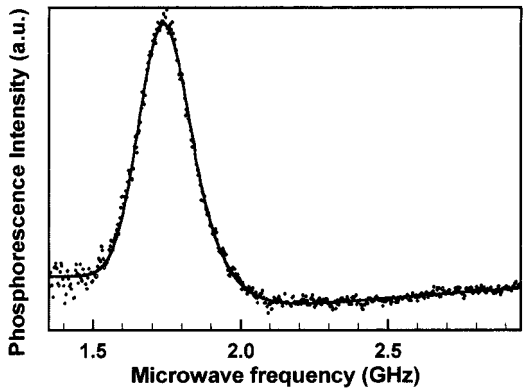

Figure 3. Delayed slow-passage ODMR spectrum of the $D-E$ transition of tryptophan in the KWK complex with poly U. Excitation was at 297 nm with 16 nm bandwidth, and emission was monitored at 412.9 nm with 3.2 nm bandwidth. Microwave sweep rate is 40 MHz/s, and $t_0 = 10$ s. Superimposed solid line represents the best fit of the response to ν_0 and $\nu_{1/2}$ given in Table 1. The fitting procedure is described elsewhere.[41]

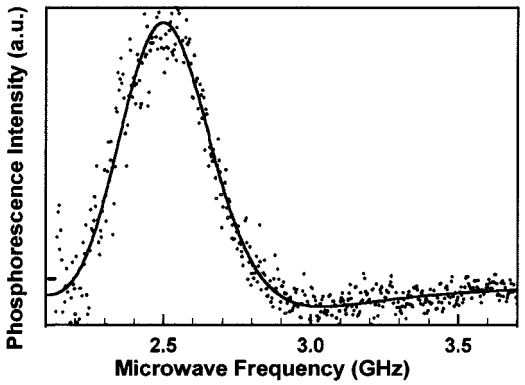

Figure 4. Delayed slow-passage ODMR spectrum of the $2E$ transition of tryptophan in the KWK complex with poly U. All conditions are the same as in the Figure 3 caption. Superimposed solid line represents the best fit of the response to ν_0 and $\nu_{1/2}$ given in Table 1, using the procedure described elsewhere.[41]

line is a least-squares fitting[41] that yields values of ν_0 and $\nu_{1/2}$. A typical delayed slow-passage ODMR spectrum of the $2E$ transition of this sample is shown in Figure 4, along with the superimposed least-squares fitting,[41] as with the $D-E$ transition. The values of ν_0 and $\nu_{1/2}$ are listed in Table 1 for the tryptophan-containing peptides, along with those for their polynucleotide complexes. The ODMR data for the MeW-containing peptides and their complexes are found in Table 2. The frequencies and bandwidths reported represent the average of four to five measurements with differing microwave sweep rate and t_0. The standard deviations reported are determined largely by the variance of each data set. The zfs parameters, D and E, are calculated from the ν_0 values of the $D-E$ and $2E$ bands of W or from the $D-E$ and $D+E$ bands of MeW.

Kinetic Parameters from MIDP. Typical MIDP data sets are shown for the $D-E$ and $2E$ transitions of the KWK complex with poly dT in Figure 5. The superimposed solid lines are the calculated responses from global analysis using least-squares minimization[40] that yield the kinetic parameters that are listed for this complex in Table 3. The kinetic parameters for the W-containing peptides and their polynucleotide complexes are listed in Table 3, while those for the MeW-containing peptides and their complexes are reported in Table 4.

Discussion

Phosphorescence and ODMR Spectra. Complex formation with each polynucleotide is accompanied by a redshift of the phosphorescence of the free peptide. These shifts result from interactions with the polynucleotide substrate that affect the energies of the ground state and triplet state differently. These interactions can be classified roughly in terms of (a) local electric fields caused by charged atoms, electric dipoles, etc.; (b) reactive electric fields induced in polarizable atoms and groups; and (c) London dispersion forces associated with aromatic stacking interactions with nucleic acid bases. Recent calculations[44] suggest that the phosphorescent ^3L_a state of W has a dipole moment smaller than that of the ground state, although it is oriented in roughly the same direction. Thus, in a rigid polar environment in which local charges and dipoles are oriented to stabilize the ground-state charge distribution of W, we would expect the phosphorescence to be blueshifted with respect to a nonpolar but polarizable environment with its weaker dipole-induced reaction field interactions. A rigid polar environment

TABLE 4: Kinetic and Radiative Parameters of 5-Methyltryptophan Peptides and Their Polynucleotide Complexes[a]

sample	k_x (s^{-1})	k_y (s^{-1})	k_z (s^{-1})	R_{zx}	R_{yx}	W_{xy} (s^{-1})	W_{xz} (s^{-1})	W_{yz} (s^{-1})	P_x[b]	P_y[b]
K(MeW)K	0.282(7)	0.115(4)	0.005(2)	0.000(8)	0.127 (8)	0.033(2)	0.037(4)	0.027(1)	0.43	0.47
K(MeW)K + poly dT	0.390(9)	0.121(5)	0.008(3)	0.012(9)	0.146 (8)	0.038(3)	0.030(5)	0.036(1)	0.57	0.35
K(MeW)K + poly I	0.40(1)	0.163(9)	0.000(6)	0.01(1)	0.15(2)	0.047(4)	0.020(8)	0.057(2)	0.45	0.48
K(MeW)K + poly U	0.43(2)	0.17(1)	0.00(1)	0.02(2)	0.24(1)	0.031(7)	0.02(1)	0.061(3)	0.52	0.40
K(MeW*)K	0.29(2)	0.10(1)	0.016(4)	0.00(1)	0.07(1)	0.042(7)	0.04(1)	0.000(4)	0.55	0.34
K(MeW*)K + poly dT	0.395(8)	0.143(6)	0.029(5)	0.07(1)	0.18(1)	0.023(3)	0.004(5)	0.029(1)	0.60	0.32
K(MeW*)K + poly I	0.34(1)	0.114(8)	0.000(4)	0.00(1)	0.08(1)	0.102(5)	0.045(8)	0.026(2)	0.45	0.47
K(MeW*)K + poly U	0.44(1)	0.135(7)	0.007(5)	0.02(1)	0.153 (9)	0.025(4)	0.031(6)	0.025(1)	0.71	0.21

[a] Standard deviation in the last digit is given in parentheses. [b] Estimated error in P_x and P_y is ± 0.03.

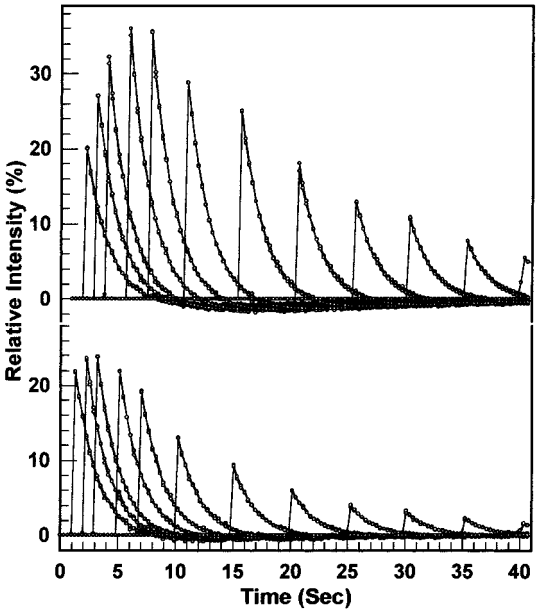

Figure 5. MIDP responses of the $D-E$ (above) and $2E$ (below) transition of tryptophan in the KWK complex with poly dT at various delay times. Superimposed solid lines are the responses calculated by global analysis[40] that yields the best-fit parameters listed in Table 3.

in which the electric field from local charges and dipoles destabilizes the ground-state charge distribution should produce a redshifted phosphorescence. London dispersion forces from aromatic stacking interactions should also lead to a redshifted phosphorescence because of the larger polarizability of the excited triplet state relative to the ground state.

The free peptide has in each case the most blue-shifted phosphorescence that we attribute to interactions of W (or MeW) with solvent dipoles in the aqueous glass that stabilize the ground state preferentially. A redshift will result from complex formation if new interactions less stabilizing to the ground state relative to the excited triplet state are introduced. These could be structurally determined electric fields less favorable to the ground state, a more polarizable local environment, and aromatic stacking interactions.

It has been shown that solvent-induced phosphorescence redshifts can be correlated linearly with reduction of the zfs D parameter.[45−47] The model for this correlation invokes the effect of the solvent electric field on the triplet state as a perturbation that admixes more highly excited *localized* triplet states with the phosphorescent state. These excited states are more diffuse, and thus D is reduced. The slope of this effect in aliphatic solvents is found[45,46] to be $\Delta D/\Delta E_{0,0} \approx 5 \cdot 10^{-6}$ for aromatic molecules such as naphthalene and quinoxaline, where $\Delta E_{0,0}$ is the phosphorescence energy shift. For W in EG-water glass, we find[48] $\Delta D/\Delta E_{0,0} \approx 3.7 \cdot 10^{-6}$. On the other hand, if we compare the zfs shifts with the phosphorescence redshifts in a series of naphthalenophanes with varying aromatic stacking geometries,[49] we find $\Delta D/\Delta E_{0,0} \approx 15 \cdot 10^{-6}$. Both ΔD and $\Delta E_{0,0}$ increase with π orbital overlap. This large value is attributed to the introduction of charge-transfer character into the triplet state as a result of stacking. The dipolar coupling introduced with the charge-transfer character contributes with opposite sign to D,[50,51] leading to abnormally large values of ΔD. It is possible to estimate the value of $\Delta D/\Delta E_{0,0}$ for tryptophan under the condition that both the zfs shift and phosphorescence shift result solely from aromatic stacking interactions with nucleobases that mix the triplet state and ground state with charge transfer states.[38] The estimate of $\Delta D/\Delta E_{0,0}$ was found to depend somewhat on the electron affinity of the base, and values between $8 \cdot 10^{-6}$ for guanine and $11 \cdot 10^{-6}$ for uracil were obtained. These values should be increased by 15−20% because the influence of charge-transfer character on D was underestimated previously.[38] Situations may occur, as discussed above, where other electrostatic interactions can selectively reduce the ground-state energy (reducing the redshift) and lead to large values of $\Delta D/\Delta E_{0,0}$ even in the absence of significant charge transfer. These situations should be characterized by relatively small values of $\Delta E_{0,0}$, however. We suggest that values of $\Delta D/\Delta E_{0,0}$ that are near 10^{-5} are diagnostic of the presence of aromatic stacking of W in nucleic acid complexes, provided $\Delta E_{0,0}$ is reasonably large (redshift ≥ 3 nm).

In comparing the phosphorescence and zfs data of the tripeptides, KWK and KW*K (Table 1), large redshifts are induced in KWK, particularly in its complexes with poly I and poly U. This shift is considerably smaller in the poly dT complex. In each case, however, $\Delta D/\Delta E_{0,0} \sim 8 \cdot 10^{-6}$, suggesting considerable aromatic stacking. The somewhat smaller redshift and D shift in the poly dT complex suggest less π-orbital overlap, possibly due to 5-methyl group repulsion of thymine. The polynucleotide complexes of KW*K, on the other hand, are characterized by much smaller redshifts and (except for poly dT) smaller D shifts. The large values of $\Delta D/\Delta E_{0,0}$ are associated with very small phosphorescence redshifts and suggest that other specific electrostatic interactions dominate in these complexes. Thus for these tripeptides, the KWK diastereomer stacks more effectively with the poly I and poly U than does KW*K.

These results are reproduced in the tripeptides K(MeW)K and K(MeW*)K, Table 2. Judging from the redshifts and D shifts, the K(MeW)K diastereomer stacks with poly I and poly U with a larger degree of π orbital overlap than does K(MeW*)K. The stacking interaction with poly dT appears to be rather small for both diastereomers, possibly for steric reasons because both aromatic residues are methylated.

When we compare the polynucleotide complexes of the tetrapeptide diastereomers, KGWK and KGW*K, we find a different situation. For a given polynucleotide complex, the redshift and the D shift are significantly larger for KGW*K than for KGWK. For each diastereomer, the value of $\Delta D/\Delta E_{0,0}$ is consistent with the dominance of aromatic stacking in inducing the shifts, but there is greater π-orbital overlap in the

KGW*K complexes. The redshift and *D* shift are too small for the poly dT complex of KGWK to be consistent with extensive aromatic stacking; on the other hand, the stacking interaction appears to be quite significant in the KGW*K complex with poly dT.

It is interesting that in the pentapeptide diastereomers KGWGK and KGW*GK, significant differences in the structure of polynucleotide complexes are detected in the triplet state properties even though the W and W* are buffered on each side by G, which does not have an asymmetric center. The relative stacking interactions are similar to those exhibited by the tetrapeptides in that for a given polynucleotide, KGW*GK exhibits a larger *D* shift and phosphorescence redshift than does KGWGK. The difference is most striking in the poly U complexes. Also, as with the tetrapeptides, the shifts exhibited in the poly dT complex of KGWGK are not consistent with significant aromatic stacking, while a fair degree of stacking is suggested in the KGW*GK complex of poly dT.

Triplet State Kinetics. The individual sublevel decay constants of the triplet state, k_i, as well as the intersystem crossing (ISC) rates that determine the relative P_i are controlled by internal spin−orbit coupling (SOC) pathways that intermix singlet and triplet character of the electronic states.[44] ISC to the $^3(\pi, \pi^*)$ state of planar aromatic molecules is known to populate the in-plane T_x and T_y sublevels preferentially.[53] This is also the case for tryptophan,[54] NCp7[54] (the 55 amino acid nucleocapsid protein of HIV-1 in which W is contained in a zinc finger motif), and the free tryptophan peptides studied here, where it is found that $P_z < P_x \sim P_y$. Sublevel-selective SOC is also manifested in the decay kinetics of W and W-containing peptides for which $k_x > k_y \gg k_z \sim 0$. See Tables 3 and 4, for example. SOC of the T_z sublevel of $^3(\pi, \pi^*)$ states is allowed only with $^1(\pi, \pi^*)$ states but the coupling is extremely inefficient.[55,56] SOC is more effective in mixing T_x and T_y with high energy $^1(\sigma, \pi^*)$ and $^1(\pi, \sigma^*)$ states leading to the weak activity of these sublevels in ISC and decay.[57] Nonplanar distortions, or other perturbations that eliminate the symmetry plane of an aromatic molecule bring about the direct mixing of π and σ orbitals and greatly increase SOC efficiency, thus enhancing the activity of T_x and T_y in ISC.[53,57]

Complex formation between the peptides and polynucleotides is accompanied by significant changes in the kinetic parameters in many cases (Tables 3 and 4). For each W-containing peptide, complex formation enhances P_x selectively so that P_x/P_y increases from <1 in the free peptide to values that are ≥2 in many complexes. We also find that k_x increases selectively in W-containing peptide complexes. However, in K(MeW)K and K(MeW*)K, complex formation leads also to larger k_y. The largest kinetic changes appear to be associated with complexes that exhibit the greatest aromatic stacking effects on *D* and $E_{0,0}$, e.g., KWK/poly I, KGW*K/poly U, KGW*GK/poly U, and K(MeW)K/poly U. We propose that the kinetic enhancements observed are the result of increased SOC in the complexes. Reduction of local symmetry produces distortions of the indole ring and allows the mixing of σ and π orbitals. Aromatic stacking interactions can cause these effects, but symmetric intercalation would tend to retain the symmetry plane of indole, and the orbital mixing (and thus SOC) will be less effective. Of course, removal of the plane of symmetry can result from other interactions such as an electric field with an out-of-plane component, or edge-to-face interactions between aromatic residues, but since they lack π orbital overlap, these will not produce large reductions of *D* and $E_{0,0}$ such as we observe in many of the complexes.

An extreme example of kinetic enhancement associated with nucleic acid binding occurs with W in position 54 of Eco SSB when the protein forms a complex with poly dT.[25,26] Although this residue in the free protein exhibits normal lifetimes and ISC pattern for W, k_x increases 4-fold to ca. 1.2 s^{-1} while $P_x/P_y > 14$ and $P_x/P_z > 25$ in the complex with poly dT. On the other hand, k_y and k_z do not increase significantly. These kinetic changes that affect the T_x sublevel selectively are accompanied by a large phosphorescence redshift, and $\Delta D = -280$ MHz is found, consistent with a large amount of charge-transfer character induced by aromatic stacking interactions. It has been shown[58] that the stacking interactions involve an additional residue, phenylalanine at position 60, which is implicated by photo-cross-linking results[59] in the binding of Eco SSB to thymine oligonucleotides.

Similar although less extreme effects of nucleic acid binding occur with W at position 37 of NCp7.[54] P_x/P_y increases from 0.84 in the free peptide to 3.0 in its complex with poly I, while k_x increases from 0.331 to 0.49 s^{-1} with no change of k_y or k_z. Complex formation between NCp7 and poly I induces a phosphorescence redshift of 6.6 nm, while $\Delta D = -94$ MHz.[36] The effects of poly I binding to NCp7 are similar to those found for poly I binding to KWK (Tables 1 and 3) suggesting similar tryptophan-base interactions in the two complexes.

Conclusions

Complex formation between four peptide diasteromer pairs—KWK, KW*K; KGWK, KGW*K; KGWGK, KGW*GK; and K(MeW)K, K(MeW*)K—and the polynucleotides poly dT, poly U, and poly I has been investigated using phosphorescence and ODMR spectroscopy. Phosphorescence redshifts and reductions of the *D* value of W and MeW are observed that vary with the polynucleotide, the peptide sequence, and the diastereomer. The largest shifts are attributed to aromatic stacking interactions between nucleic acid bases and the aromatic amino acids. When the isomer pairs are compared, the greater degree of stacking is found with KWK, K(MeW)K, KGW*K, and KGW*GK. To summarize, in the tripeptides, greater stacking is found for the L isomer, while the D isomer stacks to a greater degree in the tetrapeptide and pentapeptide.

It is of interest to compare our results with previous studies of peptide binding to nucleic acids. From their NMR measurements of the complexes of the dipeptide diastereomers KF and KF* with duplex salmon sperm DNA, Gabbay et al.[33] concluded that the phenylalanine was partially inserted between stacked bases in KF, but that it extended into the solvent in KF* Similarly, binding of K(5FW)K and K(5FW*)K to duplex DNA reveals 5FW-base interactions only with the L-isomer.[34,35] To explain their results on dipeptides and longer oligomers, Gabbay et al. proposed[33,60] a binding model in which the N-terminal lysine, utilizing its α and ϵ NH_3^+ groups binds in a stereospecific manner to the DNA backbone, directing the aromatic ring of lysylphenylalanine with the L−L designation toward the DNA helix while that of the L−D designation points outward. This binding model has been utilized to explain the results of more recent work[31,32] on binding of the peptides KWK, KGWK(O-*tert*-Bu), and KGWGK to DNA oligonucleotide hairpins and duplexes. Although these measurements were made with duplex, rather than single-stranded polynucleotides, the similarities with our measurements using single-stranded polynucleotides suggest that an analogous binding mode is utilized. In this model, the oligopeptide chain assumes a single-stranded helical β-sheet structure that can wrap around the DNA helix with L-amino acid side chains pointing alternately toward and away from the bases. We believe that this binding mode may also be utilized in peptide interactions with single-stranded polynucleotides that have a tendency to stack in helical structures. The stereospeci-

ficity is set by the binding of the amino groups of the N-terminal lysine to phosphate residues of the backbone within an essentially helical structural element of the single-stranded polynucleotide, with alternating amino acid side chains pointing toward and away from the stacked bases. Thus, in contrast with the tripeptides, the largest base−tryptophan interactions of the tetrapeptide, KGWK and pentapeptide, KGWGK should occur with the D-diastereomer, and this is what is observed. In recent ODMR studies[37] comparing the binding of KWGK and KGWK to single-stranded nucleic acids, we found larger base-stacking interactions in KWGK complexes of poly U, poly I, poly A, and $(rG)_8$. This agrees, again, with the binding model discussed above, and with previous experimental results on these tetrapeptides using fluorescence measurements.[30]

When the polynucleotide substrates are compared, the largest redshifts and *D* value shifts occur for poly U in K(MeW)K, K(MeW*)K, both tetrapeptides, and KGW*GK, while the largest shifts occur for poly I in the KWK and KW*K complexes. Poly U and poly I binding yield comparable shifts with KGWGK. The binding mode of poly dT to the peptides may differ from that of poly U and poly I since it has weaker vertical base−base interactions that would help stabilize the formation of helical regions.

The kinetic effects that are observed are not necessarily associated with aromatic stacking interactions, since they can arise from any interactions that reduce the symmetry plane of indole[53] and include edge-on interactions with bases and out of plane electric field components due to charged groups and dipoles. We do find, however, that the largest enhancements of k_x and P_x/P_y are found for the complexes KGW*K/poly U, KGW*GK/poly U, and KWK/poly I, which are among those that exhibit the largest spectral shifts attributed to aromatic stacking. The largest enhancement of decay kinetics of MeW are found in the complex K(MeW)K/poly U which also exhibits the largest spectral shifts among the MeW peptide complexes. In this case, in contrast with the W peptides, both k_x and k_y increase, and there is only a minor change in P_x/P_y. The enhancement of k_x and k_y is nearly the same in the complex K(MeW)K/poly I, although the spectral shifts are somewhat less. These results suggest that enhancement of SOC by nucleic acid binding is less selective, in general, for the T_x sublevel in MeW than in W.

Acknowledgment. We are grateful to the Camille and Henry Dreyfus Foundation for a Senior Scientist Initiative Award to A.H.M.. This publication was made possible by Grant Number ES-02662 from the National Institute of Environmental Health Sciences (A.H.M.) and by National Cancer Institute Contract N01-56000 (JRC). Its contents are solely the responsibility of the authors and do not necessarily reflect the views of the NIEHS or NCI, NIH.

References and Notes

(1) Kreil, G. *Annu. Rev. Biochem.* **1997,** *66*, 337.
(2) Dunlop, D. S.; Neidle, A.; McHale, D.; Dunlop, D. M.; Lajtha, A. *Biochem. Biophys. Res. Commun.* **1986**, *141*, 27.
(3) Hashimoto, A.; Kumashiro, S.; Nishikawa, T.; Oka, T.; Takahashi, K.; Mito, T.; Takashima, S.; Dio, N.; Mizutani, Y.; Yamazaki, T.; Kaneko, T.; Ootomo, E. *J. Neurochem.* **1993**, *61*, 384.
(4) Miller, S. L.; Orgel, L. E. *The Origins of Life on Earth*; Prentice Hall: New Jersey, 1974.
(5) Woese, C. R.; Dugre, D. H.; Dugre, S. A.; Kondo, M.; Saxinger, W. C. *Symp. Quantum Biol.* **1966**, *31*, 723.
(6) Crick, F. H. C. *J. Mol. Biol.* **1968**, *38*, 367.
(7) Mizutani, H.; Ponnamperuma, C. *Origins Life* **1977**, *8*, 183.
(8) Wickramasinghe, N. S. M. D.; Staves, M. P.; Lacey, J. C., Jr. *Biochemistry* **1991**, *30*, 2768.
(9) Lacey, J. C., Jr.; Wickramasinghe, N. S. M. D.; Sabatini, R. S. *Experimentia* **1992**, *48*, 379.
(10) Gabbay, E. J.; Kleinman, R. *J. Am. Chem. Soc.* **1967**, *89*, 7123.
(11) Deranleau, D. A. *J. Am. Chem. Soc.* **1969**, *91*, 4044.
(12) Reuben, J. *FEBS Lett.* **1978**, *94*, 20.
(13) Hui Bon Hoa, G.; Montenay-Garestier, T.; Hélène, C. *Nature (London)* **1968**, *223*, 1061.
(14) Montenay-Garestier, T.; Hélène, C. *Biochemistry* **1971**, *10*, 300.
(15) Wagner, T. E. *Nature (London)* **1969**, *222*, 1170.
(16) Smythies, J. R.; Antun, F. *Nature (London)* **1969**, *223*, 1061.
(17) Hélène, C. *Nature New Biol. (London)* **1971**, *234*, 120.
(18) Raszka, M.; Mandel, M. *Proc. Natl. Acad. Sci. U.S.A.* **1971**, *86*, 1190.
(19) Brun, F.; Toulmè, J. J.; Hélène, C. *Biochemistry* **1975**, *14*, 558.
(20) Porschke, D.; Ronnenberg, J. *Biophys. Chem.* **1981**, *13*, 283.
(21) Durand, M.; Maurizot, J.-C.; Borazan, H. N.; Hélène, C. *Biochemistry* **1975**, *14*, 563.
(22) Gabbay, E. J.; Sanford, K.; Baxter, C. S. *Biochemistry* **1972**, *11*, 3429.
(23) Dimicoli, J.-L.; Hélène, C. *Biochemistry* **1974**, *13*, 714; 724.
(24) Co, T.-t.; Maki, A. H. *Biochemistry* **1978**, *17*, 182.
(25) Zang, L.-H.; Maki, A. H.; Murphy, J. B.; Chase, J. W. *Biophys. J.* **1987**, *52*, 867.
(26) Tsao, D. H. H.; Casas-Finet, J. R.; Maki, A. H.; Chase, J. W. *Biophys. J.* **1989**, *55*, 927.
(27) Mascotti, P. D.; Lohman, M. T. *Biochemistry* **1992**, *31*, 8932.
(28) Mascotti, P. D.; Lohman, M. T. *Biochemistry* **1997**, *36*, 7272.
(29) Rajeswari, M. R.; Montenay-Garestier, T.; Hélène C. *Biochemistry* **1987**, *26*, 6825.
(30) Montenay-Garestier, T.; Takasugi, M.; Le Doan, T. In *Nucleic Acids: The Vectors of Life*; Pullman, B., Jortner, J., Eds.; Reidel: Dordrecht, 1983; p 305.
(31) Rajeswari, M. R.; Bose, H. S.; Kukreti, S.; Gupta, A.; Chauan, V. S.; Roy, K. B. *Biochemistry* **1992**, *31*, 6237.
(32) Roy, K. B.; Kukreti, S.; Bose, H. S.; Chauan, V. S.; Rajeswari, M. R. *Biochemistry* **1992**, *31*, 6341.
(33) Gabbay, E. J.; Adawadkar, P. D.; Wilson, W. D. *Biochemistry* **1976**, *15*, 146.
(34) Shine, N. R.; James, T. L. *Biochemistry* **1985**, *24*, 4333.
(35) Shine, N. R.; Bubienko, E.; James, T. L. *Biochemistry* **1985**, *24*, 4341.
(36) Wu, J. Q.; Ozarowski, A.; Maki, A. H.; Urbaneja, M. A.; Henderson, L. E.; Casas-Finet, J. R. *Biochemistry* **1997**, *36*, 12506.
(37) Misra, A.; Ozarowski, A.; Casas-Finet, J. R.; Maki, A. H. *Biochemistry* **2000**, *39*, 13772.
(38) Maki, A. H.; Ozarowski, A.; Misra, A.; Urbaneja, M. A.; Casas-Finet, J. R. *Biochemistry* **2001**, *40*, 1403.
(39) Wu, J. Q.; Ozarowski, A.; Maki, A. H. *J. Magn. Reson. A* **1996**, *119*, 82.
(40) Ozarowski, A.; Wu, J. Q.; Maki, A. H. *J. Magn. Reson. A* **1996**, *121*, 178.
(41) Wu, J. Q.; Ozarowski, A.; Davis, S. K.; Maki, A. H. *J. Phys. Chem.* **1996**, *100*, 11496.
(42) Smith, C. A.; Maki, A. H. *J. Phys. Chem.* **1993**, *97*, 997.
(43) Schmidt, J.; Veeman, W. S.; van der Waals, J. H. *Chem. Phys. Lett.* **1968**, *4*, 341.
(44) Hahn, D. K.; Callis, P. R. *J. Phys. Chem. A* **1997**, *101*, 2686.
(45) van Egmond, J.; Kohler, B. E.; Chan, I. Y. *Chem. Phys. Lett.* **1975**, *34*, 423.
(46) Gradl, G.; Friedrich, J.; Kohler, B. E. *J. Chem. Phys.* **1986**, *84*, 2079.
(47) Williamson, R. L.; Kwiram, A. L. *J. Chem. Phys.* **1988**, *88*, 6092.
(48) von Schütz, J. U.; Zuclich, J.; Maki, A. H. *J. Am. Chem. Soc.* **1974**, *96*, 714.
(49) Haenel, M. W.; Schweitzer, D. *Adv. Chem. Ser.* **1988**, *217*, 333.
(50) Hayashi, H.; Iwata, S.; Nagakura, S. *J. Chem. Phys.* **1969**, *50*, 993.
(51) Keijzers, C. P.; Haarer, D. *J. Chem. Phys.* **1977**, *67*, 925.
(52) van der Waals, J. H.; de Groot, M. S. In *The Triplet State*; Zahlan, A. B., Ed.; Cambridge University Press: Cambridge, 1967; p 101.
(53) El Sayed, M. A.; Moomaw, W. R.; Chodak, J. B. *Chem. Phys. Lett.* **1973**, *20*, 11.
(54) Ozarowski, A.; Maki, A. H. *J. Magn. Reson.* **2001**, *148*, 419.
(55) Weissman, S. I. *J. Chem. Phys.* **1950**, *18*, 232.
(56) McClure, D. S. *J. Chem. Phys.* **1952**, *20*, 682.
(57) Lower, S. K.; El Sayed, M. A. *Chem. Rev.* **1966**, *66*, 199.
(58) Casas-Finet, J. R.; Khamis, M. I.; Maki, A. H.; Chase, J. W. *FEBS Lett.* **1987**, *220*, 347.
(59) Merrill, B. M.; Williams, K. R.; Chase, J. W.; Konigsberg, W. H. *J. Biol. Chem.* **1984**, *259*, 10850.
(60) Gabbay, E. J.; Adawadkar, P. D.; Kapicak, L.; Pearce, S.; Wilson, W. D. *Biochemistry* **1976**, *15*, 152.